# Conditioning the probability field of facies to facies observations using a regularized Element-Free Galerkin (EFG) method

Sebacher, B.; Hanea, R.; Marzavan, S.

**DOI**
10.3997/2214-4609.201902249

**Publication date**
2019

**Document Version**
Final published version

**Published in**
4th EAGE Conference on Petroleum Geostatistics

FAULT&TOPSEALS PALERMO•2019

EAGE

WeP05

# Imbricated Structure and Hydraulic Path Induced by Strike Slip Reactivation of a Normal Fault in Carbonates

I. Aubert[1]*, J. Lamarche[1], P. Richard[2], P. Leonide[1]

[1] Aix Marseille Univ, CNRS, IRD, CEREGE; [2] Shell Global Solutions International BV

## Summary

Fault zones strongly impact basin reservoir properties as they can act as drains or barriers depending of their structural and diagenetic properties. In the case of reactivated faults, newly develop fracture and fault systems reworked and cross-cut preexisting structures generated by the first fault activity potentially result in new fluid pathways. The study focalized on the polyphase Castellas fault affecting Barremian calcarenites (Urgonian facies). We performed a 870m-long high resolution mapping along the Castellas fault zone with a data of 586 measurements, including 56 fault planes, 460 fractures and 70 bedding planes. We realized a geological map and a stratigraphic log and fifteen cross-sections perpendicular to the fault zone, to capture fault architecture variations. The Castellas fault structure, observed on map and cross-sections exhibit large lateral variations of fault core and fault geometry. It is composed of a complex anastomosed architecture made of 8 main fault planes striking from N047° to N078°, with secondary fault planes, horse tail structures and imbricated lenses. Fault zone hydraulic signature change from a porous fault rock with a tight damage zone during normal faulting to a fracture network and fault core enhanced permeability during strike-slip deformation.

## Introduction

Fault zones strongly impact basin reservoir properties as they can act as drains or barriers (Tondi 2007; Agosta et al. 2010; Matonti et al. 2012; Huisman 2016; Sinisi et al. 2016) depending of their structural and diagenetic properties . In the case of reactivated faults, newly develop fracture and fault systems reworked and cross-cut preexisting structures generated by the first fault activity and potentially result in new fluid pathways. Hence, fault reactivation can strongly alter the architecture of primary fault zones as well as their hydraulic properties. To understand the impact of structural inheritance on hydraulic properties of multiphase faults, we have targeted the Castellas fault zone located in La Fare anticlinal (Provence – SE France, Fig. 1). It has affected Barremian calcarenites of the Urgonian facies. The structure of this fault trending N060 to N070 dipping of 40° to 80°N, results from two tectonic events since early Barremian (Matonti et al. 2012): a mid-cretaceous Durancian uplift leading to the creation of a normal fault and a Pyreneo-Provençal and Alpine shortenings triggering reactivation in strike-slip.
Our analysis has focused first on the characterization of the structural pattern related to each deformation event, to then determine the impact of structural inheritance during the strike-slip reactivation. Finally, we attempt to estimate the hydraulic behavior of the fault zone.

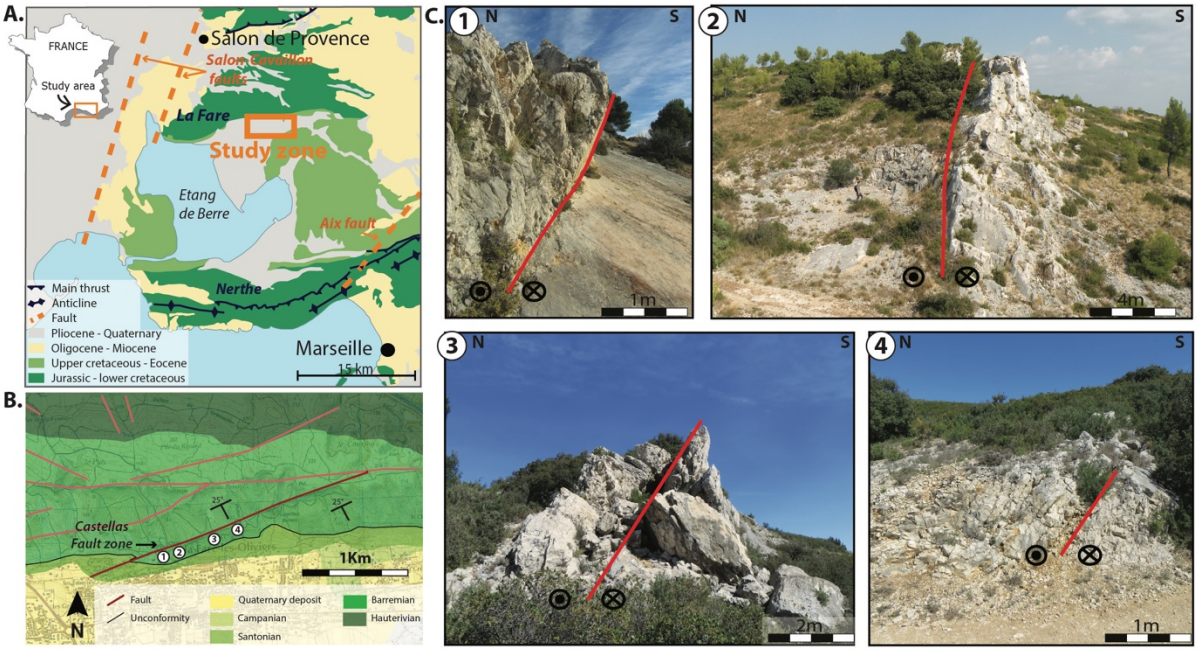


***Figure 1*** *A. Geological context of Castellas fault zone B. Simplified structural map of the study area and C. pictures of Castellas fault, localized on map B.*

## Methods

To fully characterize the fault zone lateral geometry, we performed a 870m-long high resolution mapping along the Castellas fault zone. We measured all major an subordonate faults, breccias, fracture patterns and bedding surfaces.
The data base comprises 586 measurements, including 56 fault planes, 460 fractures (432 joints, 28 fractures filled with oxides) and 70 bedding planes.
To decipher the role played by carbonate facies on the fault architecture, we realized a geological map and a stratigraphic log considering the sedimentary content and the depositional texture according to the Dunham classification (Dunham 1962). Fifteen cross-sections have been elaborated along and perpendicular to the fault zone, to capture the variations of fault architecture and fault core, as well as the characteristics of damage zones and fracture networks.

## Fault architecture

The fault zone is composed of 8 anastomosed main fault planes striking from N047° in the western part of the fault, to N078° in the eastern part of the fault (Fig. 2A). The main fault planes are 30 to 330 meters long. Fault segments can be joined and coalescent or non-connected (Fig. 2B). Subordinate minor branch-faults are sub-parallel to the main fault axis. Converging faults form lenses while diverging faults form pseudo-splay structures. In lenses and in the damage zone, fractures compose a complex pattern.

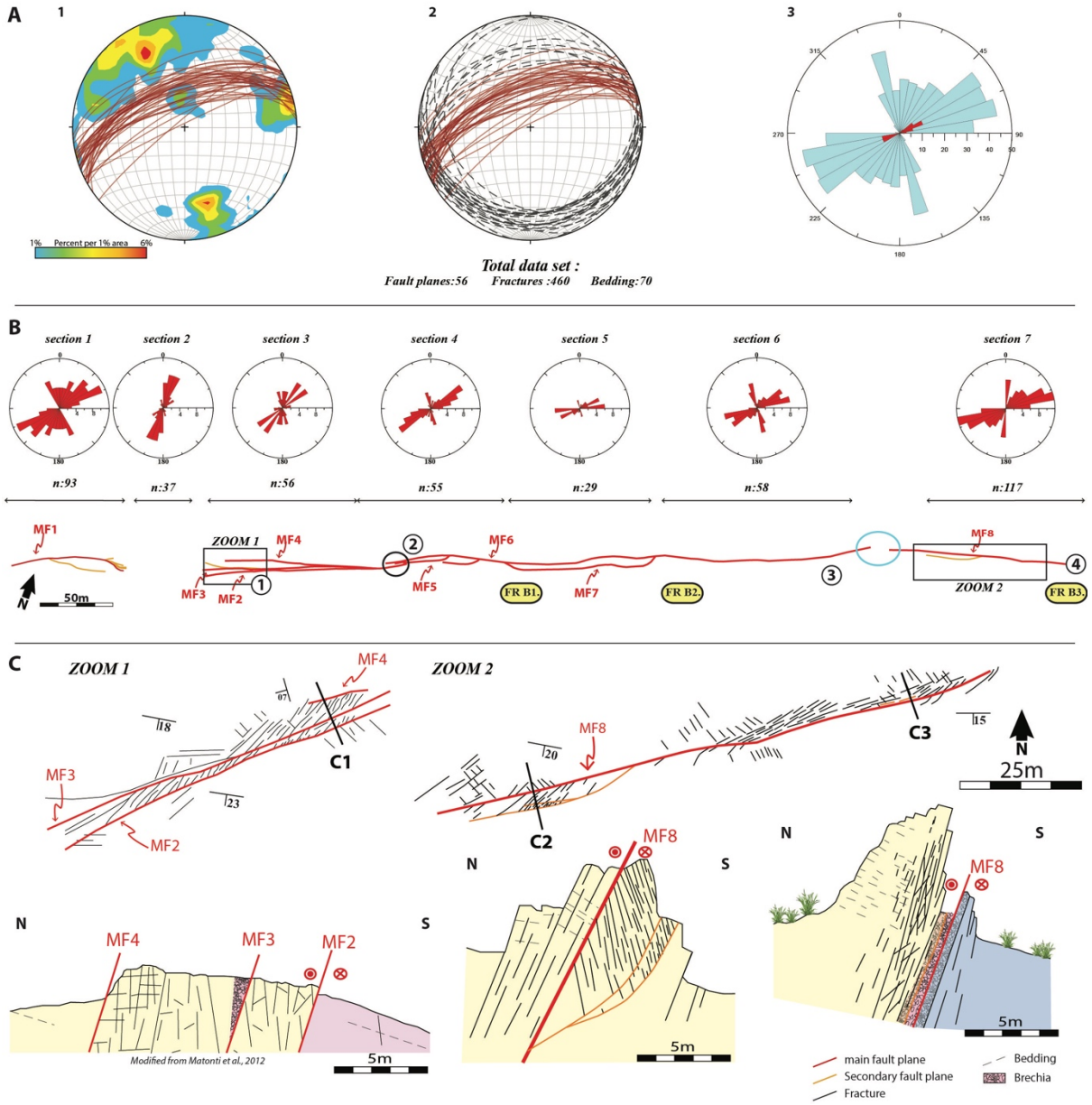


***Figure 2*** *Architecture of the Castellas fault zone. A: Stereographic projection of the bulk data using OSXStereonet 10.2.8 (Allmendinger et al. 2013; Cardozo and Allmendinger 2013) :A1&A2: fracture density contoured poles, faults (red lines) and bedding (dashed lines) ; A3: Fracture (blue) and fault planes(red) strikes as rose diagram, B: simplified structural map of fault with sections 1 to 7 fracture strikes as rose diagrams (red: main fault planes orange: secondary fault planes,) coalescent segments and unconnected segments are respectively circled of black and blue, C. High resolution structural map of 2 fault zone sections and three cross sections in areas 1 and 2.*

Fractures have been sorted in 3 sets: N020, N065 and N165.

- The set N020° is mainly observed in sector 2 (label 2 on Fig. 2B)
- The sets N065° and N165° occur all along main fault planes.

Overall, fault core along strike is heterogeneous and discontinuous. Its thickness ranges from 0 to 1m. The fault core is constituted by two fault rocks (Fig. 3): A cohesive and an un-cohesive breccia. The cohesive breccia is composed of sub-rounded to rounded clasts surrounded of a grey matrix (<30%) named Fault rock 1 (FR1, on Fig. 3B). This breccia has been interpreted as being related to the normal activity during Durancian uplift. The un-cohesive breccia with angular to sub-rounded clasts surrounded by an orange/oxided matrix named Fault rock 2 (FR2, on Fig. 3B). This breccia has been interpreted as being linked to the strike-slip reactivation during Pyrenean shortening. FR2 present less deformed facies constituted of angular clasts with a low proportion of matrix (<5%) and more deformed facies composed of sub-rounded to rounded clasts with a higher proportion of matrix (>20%).

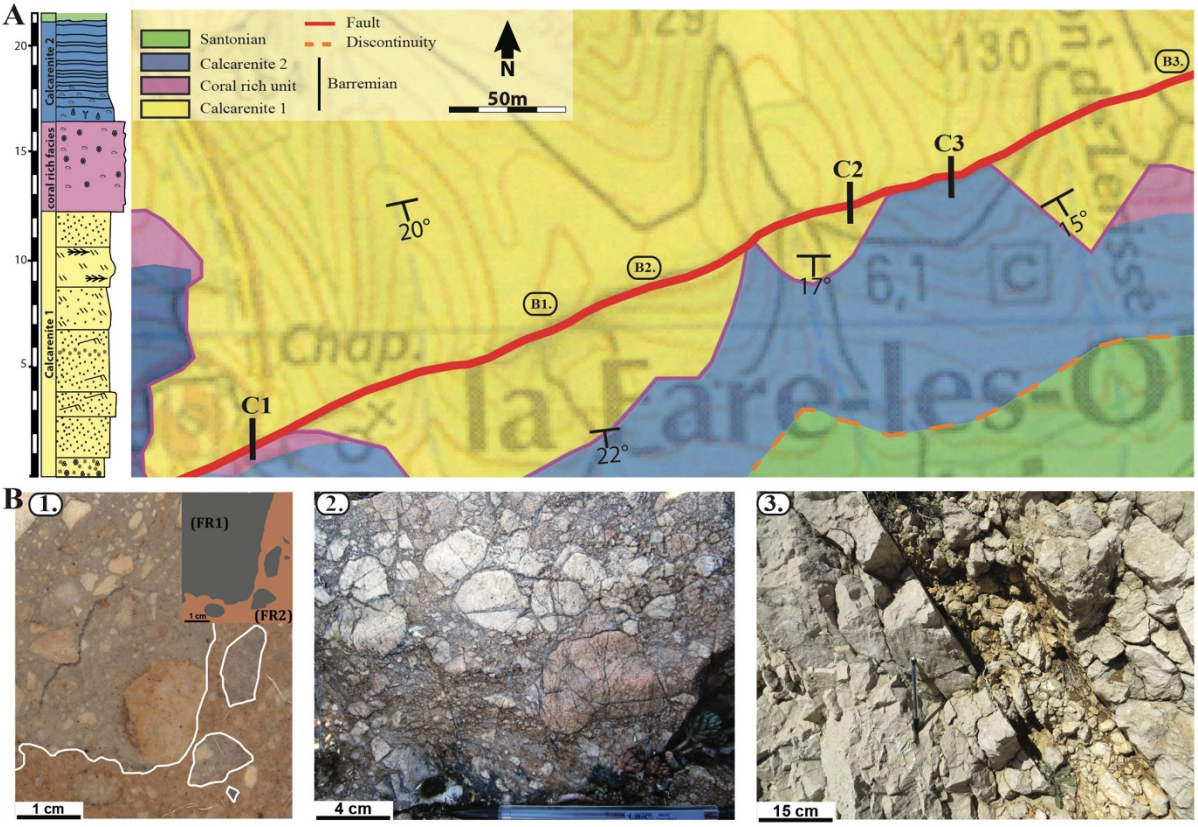


***Figure 3*** *A. Geological map of the fault zone pointing out facies juxtapositions and B. Pictures of fault rock 1 (FR1 on B1, B2) and fault rock 2 (FR2 on B1, B3) Picture localization is indicated on Fig. 2B.*

## Conclusion

The structure of the Castellas fault, observed on map and cross-sections exhibit large lateral variations of fault core and fault geometry (Fig. 2 and Fig 3). It is composed of a complex anastomosed architecture made of 8 main fault planes (along the mapped interval), with secondary fault planes, horse tail like structures and imbricated lenses. The overall fault architecture is neither conventional for strike-slip nor for normal faults. We relate the peculiar structure of the fault to

- The strike-slip reactivation of a pre-existing normal fault
- Coalescence of several fault segments during fault evolution (Filbrandt et al. 2007)
- The juxtaposition of 3 different carbonate facies with different mechanical properties
- The mechanical inheritance due to carbonate diagenesis associated to the first fault activation.

The Castellas fault architecture and properties provide a good analogue for sub-surface carbonate reservoirs which have undergone either part or the same complete complex structural evolution.
The hydraulic signature of such a fault is neither a drain nor a seal, but a sieve. The phase of normal faulting has preferentially generated a porous fault rock with a tight damage zone while the strike-slip deformation has preferentially enhanced permeability fracture network and fault core. We will provide more detailed evidence of the conclusions above during the presentation.

**References**

Agosta, F., Alessandroni, M., Antonellini, M., Tondi, E. & Giorgioni, M. [2010]. From fractures to flow: A field-based quantitative analysis of an outcropping carbonate reservoir. *Tectonophysics*, **490**, 197–213.

Allmendinger, R.W., Cardozo, N. & Fisher, D.M. [2013]. Structural geology algorithms: Vectors and tensors. *Cambridge University Press*, **9781107012**, 1–289.

Cardozo, N. & Allmendinger, N.W. [2013]. Sperical projections with OSXStereonets. *Computers & Geosciences*, **51**, 193–205.

Dunham, R.J. [1962]. Classification of Carbonate Rocks According to Depositional Textures. *Classification of Carbonate Rocks--A Symposium*, **1**, 108–121.

Filbrandt, J.B., Richard, P.D. & Franssen, R. [2007]. Fault growth and coalescence: Insights from numerical modelling and sandbox experiments. *GeoArabia*, **12**, 17–32.

Huisman, J.G.S. and B.A.H. [2016]. Toward the creation of models to predict static and dynamic fault-seal potential in carbonates.

Matonti, C., Lamarche, J., Guglielmi, Y. & Marié, L. [2012]. Structural and petrophysical characterization of mixed conduit/seal fault zones in carbonates: Example from the Castellas fault (SE France). *Journal of Structural Geology*, **39**, 103–121.

Sinisi, R., Petrullo, A.V., Agosta, F., Paternoster, M., Belviso, C. & Grassa, F. [2016]. Contrasting fault fluids along high-angle faults: a case study from Southern Apennines (Italy). *Tectonophysics*, **690**, 206–218.

Tondi, E. [2007]. Nucleation, development and petrophysical properties of faults in carbonate grainstones: Evidence from the San Vito Lo Capo peninsula (Sicily, Italy). *Journal of Structural Geology*, **29**, 614–628.